

Published in final edited form as:

Acad Radiol. 2007 April ; 14(4): 431–436.

Volumetric Assessment of Tumor Infiltration of Adjacent White Matter Based on Anatomic MRI and Diffusion Tensor Tractography

Ion-Florin Talos, M.D.^{1a}, Kelly H. Zou, Ph.D.¹, Ron Kikinis, M.D.¹, and Ferenc A. Jolesz, M.D.¹

¹Department of Radiology, Brigham and Women's Hospital, Harvard Medical School, Boston, MA, USA

Abstract

Rationale and Objectives—To perform a retrospective, quantitative assessment of the anatomic relationship between intra-axial, supratentorial, primary brain tumors, and adjacent white matter fiber tracts, based on anatomic and diffusion tensor MRI. We hypothesized that white matter infiltration may be common among different types of tumor.

Material and Methods—Preoperative, anatomic (T1- and T2-weighted) and LINESCAN diffusion tensor MRI were obtained in 12 patients harboring supratentorial gliomas (WHO grade II and III). The two imaging modalities were rigidly registered. The tumors were manually segmented from the T1- and T2- weighted MRI, and their volume calculated. A three-dimensional tractography was performed in each case. A second segmentation and volume measurement was performed on the tumor regions intersecting adjacent white matter fiber tracts. Statistical methods included summary statistics to examine the fraction of tumor volume infiltrating adjacent white matter.

Results—There were five patients with low-grade oligodendroglioma (WHO grade II), one with low-grade mixed oligoastrocytoma (WHO grade II), one with ganglioglioma, two with low-grade astrocytoma (WHO II), and three with anaplastic astrocytoma (WHO grade III). We identified white matter tracts infiltrated by tumor in all 12 cases. The median tumor volume (\pm standard deviation) in our patient population was 42.5 ± 28.9 ml. The median tumor volume (\pm standard deviation) infiltrating white matter fiber tracts was 5.2 ± 9.9 ml. The median percentage of tumor volume infiltrating white matter fiber tracts was $21.4 \% \pm 9.7 \%$.

Conclusions—The information provided by diffusion tensor imaging combined with anatomic MRI might be useful for neurosurgical planning and intraoperative guidance. Our results confirm previous reports that extensive white matter infiltration by primary brain tumors is a common occurrence. However, prospective, large population studies are required to definitively clarify this issue, and how infiltration relates to histologic tumor type, tumor size and location.

Keywords

Brain tumor; diffusion tensor imaging; anatomic MRI; 3D-tractography; tumor infiltration of white matter

aCorrespondence to: Ion-Florin Talos, M.D., Instructor in Radiology, Brigham and Women's Hospital, Harvard Medical School, 75 Francis St., Boston, MA 02115, USA, Phone: 617-732-5623, Fax: 617-582-6033, e-mail: talos@bwh.harvard.edu.

Publisher's Disclaimer: This is a PDF file of an unedited manuscript that has been accepted for publication. As a service to our customers we are providing this early version of the manuscript. The manuscript will undergo copyediting, typesetting, and review of the resulting proof before it is published in its final citable form. Please note that during the production process errors may be discovered which could affect the content, and all legal disclaimers that apply to the journal pertain.

Introduction

According to the Central Brain Tumor Registry of the United States, the incidence of primary benign and malignant brain tumors in this country is 14.1 patients per 100,000 individuals per year (6.8 per 100,000 individuals per year for low-grade tumors, and 7.3 per 100,000 individuals per year for malignant tumors) [1].

The survival of patients harboring primary brain tumors appears to be influenced by a variety of factors, such as age, histologic tumor type, gender, preoperative Karnofsky performance score, epilepsy as presenting symptom, tumor involvement of the contralateral hemisphere, and extent of tumor resection [2,3]. Surgical resection plays an important role in the management of both low- and high-grade primary brain tumors. Although no prospective randomized outcome study has been conducted to date, retrospective data suggest an association between gross total tumor resection and increased overall survival [4–6].

The goal of surgical treatment is to remove as much tumor tissue as possible, while in the same time preserving the integrity of functionally eloquent gray and white matter structures, and thus avoid postoperative neurologic deficits. However, tumor infiltration of eloquent cortical areas and/or white matter tracts may preclude safe gross total resection. Consequently, knowledge of the relationship between tumor and eloquent cortical and white matter regions might be helpful for preoperatively determining the extent to which a brain tumor can be surgically removed, and also for guiding the actual surgical procedure.

By taking advantage of the anisotropic diffusion pattern of water molecules in highly structured tissues, such as the cerebral white matter, DT-MRI provides a fully non-invasive method for in vivo visualization of white matter fiber tracts under normal and pathologic conditions [7–9]. During the past few years, several studies investigating tumor-induced alterations of cerebral white matter [10–13] and patterns of tumor invasion [14] have been published. To our knowledge, however, none of these groups attempted a volumetric assessment of the extent of tumor infiltration of adjacent white matter.

Therefore, the purpose of the present study was to perform a preliminary quantitative assessment of white matter infiltration by primary brain tumors. We hypothesized that white matter infiltration may be common among different types of tumors.

Materials and Methods

Patient Population

Twelve consecutive patients with intracerebral supratentorial mass lesion satisfying the radiological criteria for low- or high-grade glial neoplasm were selected for this retrospective study. Based on previous anatomical MRI exams, it was estimated that the lesions were located in close proximity to eloquent cortical areas (e.g. primary and supplementary motor cortex, speech cortices), and white matter tracts (e.g. corticospinal tract, optic radiation) (Table 1), and consequently all patients in this series underwent preoperative LINESCAN diffusion tensor MRI (DT-MRI) as part of surgical planning for image-guided tumor resection, in addition to preoperative anatomic T2-weighted fast spin echo (T2FSE), and volumetric T1-weighted MRI (3D-SPGR). There were 7 female and 5 male patients. The mean age was 46.7 years (range 17–64 years). All patients in this series underwent image-guided tumor resection. Histopathologic examination of the resected tumor tissue confirmed the diagnosis of low- or high-grade glioma in each case. This retrospective study was approved by the hospital's Internal Review Board, and the requirement for informed consent was waived.

Image Acquisition

All imaging studies were performed on a GE Signa MRI-scanner, with a field strength of 1.5 Tesla.

Anatomic imaging included the following sequences:

1. Whole brain T2-weighted fast spin echo: 5mm axial slices, TE/TR=100/3000 msec, FOV=22 cm, matrix 256×192, and
2. Whole brain 3D-SPGR (Spoiled Gradient Echo Recall) with and without contrast: whole brain 3D-SPGR (spoiled gradient echo recall) series with 1.5 mm axial slices, TE/TR=6/35 msec, flip angle=75°, FOV=24 cm, matrix 256×256.

Diffusion tensor imaging: axial and coronal line scan diffusion images (TE=64 msec, TR=2592 msec, slice thickness 4 mm) were acquired, covering the entire tumor and adjacent healthy brain parenchyma, as well as the brainstem and basal ganglia regions. Each section from the DT-MRI sequence was acquired from six non-collinear gradient directions. In addition, a baseline T2-weighted slice was acquired for each section.

Image Analysis

The 3D-Slicer software package [15] was used for image registration and processing. This is a modular software package with image registration, segmentation and DT-MRI processing capabilities.

First, the anatomic (3D-SPGR and T2-FSE) and the DT-MRI scans were rigidly registered, using a maximization of mutual information (MI) algorithm [16]. This algorithm is fully implemented in the 3D-Slicer software package, and it is known to provide robust and accurate results [16,17]. The registration results were inspected by three raters (IFT, FAJ, and RK, with 15, 35, and 24 years of experience in neuroimaging), and manual adjustments were made where necessary, using as reference anatomic landmarks such as the anterior and posterior commissures, lateral ventricles, and corpus callosum.

Each tumor was manually segmented (outlined) from the anatomic T2-FSE scans using the 3D-Slicer and a computer mouse. The apparent tumor boundaries were determined by consensus between three raters (IFT, FAJ, and RK). According to the literature, among anatomic MRI modalities, T2-weighted images appear to reflect the tumor extent more closely, although occult tumor can be found even beyond the region of increased T2-signal in some gliomas [18–22]. The tumor volume was computed from the segmented area and voxel size, using the 3D-Slicer software.

In the next step, the white matter structure from DT-MRI was visualized. First, fractional anisotropy maps were generated in each case, using the 3D-Slicer software. Next, we obtained both a 2D-visualization (headless arrows to represent the in-plane component of the principal eigenvector along with a color-coded out-of-plane component) [23] and a 3D-tractography in each patient. For the 3D-tractography, we used the algorithm described by Westin et al. [24], which is fully implemented in the 3D-Slicer package. In order to calculate the trajectory of fiber tracts, this algorithm takes into account fractional anisotropy, as well as the angle between the primary eigenvector within a voxel and the equivalent vector in the neighboring voxels. In order to selectively visualize each fiber tract expected to be in close spatial relationship with the tumor (based on anatomic MRI), we defined seed points, from which the tractography was initialized: ventral brainstem for reconstructing the corticospinal tract, the white matter region adjacent to the lateral geniculate body for the optic radiation, the temporal lobe stem for tracking the uncinate fasciculus, etc. The 3D-tractography results were compared with the

corresponding 2D-visualization maps and manually corrected, in order to insure that artifacts were removed.

Finally, the tumor regions intersecting white matter tracts were manually segmented and their volume calculated in the same manner as the total tumor volume.

Statistical methods included summary statistics to examine the fraction of tumor volume infiltrating adjacent white matter.

Results

There were five patients with low-grade oligodendroglioma (WHO grade II), one with low-grade mixed oligoastrocytoma (WHO grade II), one with ganglioglioma, and two with low-grade astrocytoma and three with anaplastic astrocytoma (WHO grade III) (Table 1).

Nine tumors were confined to a single cerebral lobe (six frontal, two temporal, one occipital), whereas three tumors involved more than one lobe (two fronto-parietal, one fronto-temporal) (Table 1).

We identified tumor infiltrated white matter tracts in all cases, irrespective of histopathological diagnosis and grading (Figure 1, Figure 2, Figure 3). In addition to infiltration, fiber tract displacement was also observed in most patients (Figure 1).

Apparent mass effect on the anatomic scans did not exclude white matter tract infiltration (Figure 2).

The median tumor volume (\pm standard deviation) in our patient population was 42.5 ± 28.9 ml. The median tumor volume (\pm standard deviation) infiltrating white matter fiber tracts was 5.2 ± 9.9 ml. Expressed as percentage of the median total tumor volume, the fraction of tumor volume infiltrating white matter fiber tracts was $21.4 \% \pm 9.7 \%$. The results of the volumetric analysis are presented in Table 2.

A systematic analysis of patient outcomes and how they may relate to the availability of DT-MRI data in this small retrospective series is beyond the scope of present study. However, we believe that the information provided by DT-MRI can potentially help to further improve surgical outcomes of brain tumor patients. We illustrate this point using data from two cases in our series.

In the case of a 62 year old female patient with left frontal low-grade oligodendroglioma (Case 3, Table 1), the tractography identified corticospinal fibers in the anterior portion of the tumor (Figure 2). Since the imaging findings suggested that this tumor-infiltrated fiber contingent originated in the supplementary, and not the primary motor cortex, it was decided to proceed aggressively and perform gross total tumor resection. Postoperatively, the patient developed a supplementary motor area syndrome, with contralateral hemiplegia and aphasia, which completely resolved during the first three months post-surgery.

In the case of a 23 year old male patient with insular ganglioglioma (Case 8, Table 1), the anatomic T1- and T2-weighted imaging demonstrated a round, non-enhancing tumor mass in the right insula, compressing the right optic tract and right cerebral peduncle. In addition to these findings, the DT-MRI demonstrated partial tumor infiltration of the right corticospinal tract (Figure 2). The patient underwent craniotomy and tumor resection with intraoperative MRI-guidance, under local anesthesia and conscious sedation. As the resection approached the medial aspect of the tumor, where the presence of infiltrated corticospinal fibers was suspected (based on the DT-MRI findings), the patient developed a transient contralateral hemiparesis.

A small medial tumor remnant was left in place, in order to avoid injury to the corticospinal tract. The hemiparesis completely resolved within three days post-surgery.

Discussion

Intraoperative cortical stimulation studies, and more recently magnetic source imaging (MSI) have demonstrated that functioning cortical tissue may be preserved within primary brain tumors, even in areas appearing grossly abnormal at visual inspection [25,26].

In the pre-DT-MRI era, some intraoperative white matter stimulation studies suggested that preserved white matter tracts may be present within some gliomas [27]. The advent of DT-MRI has enabled in vivo, non-invasive studies of tumor-induced white matter changes [10–13], and patterns of tumor invasion [14]. Furthermore, DT-MRI is being increasingly used for guiding surgical procedures [28]. However, to our knowledge, there is no prior study attempting a volumetric assessment of the extent of white matter infiltration by primary brain tumors.

We have shown that, by combining the information provided by anatomic and diffusion tensor MRI, it is possible to quantify the extent of tumor infiltration of adjacent white matter. Such a quantitative measure may help improve the accuracy of currently available predictive models for brain tumor resectability [29].

A systematic analysis of patient outcomes and how they may relate to the availability of DT-MRI data in this small retrospective series is beyond the scope of present study. However, we believe that the information provided by DT-MRI can potentially help to further improve surgical outcomes of brain tumor patients, and we illustrated this point at the example of two cases from our series.

Our results confirm existing information that tumor infiltration is a common occurrence among different histologic brain tumor types, and that the fraction of tumor volume infiltrating white matter tracts may be in some cases as significant as to preclude safe gross total tumor resection. Also, our preliminary results indicate that the information provided by anatomic MRI scans may not always be sufficient for assessing tumor resectability, and for surgical navigation, since even tumors displaying prominent mass effect on anatomic MRI may, at the same time, infiltrate adjacent white matter tracts.

Our retrospective study is limited by the relatively small sample size. Furthermore, no histological validation of the DT-MRI results was obtained in this patient group. Also, this small included only patients with tumors located in close proximity to eloquent cortical and white matter structures, which may have introduced a bias. Finally, it is possible that some intact fibers in the tumor periphery may have remained undetected by tractography, due to tumor-induced alterations of tissue anisotropy.

Although our preliminary results confirm the results of previously published studies that white matter infiltration by primary brain tumors is a common occurrence, prospective, large population studies are required in order to definitively clarify this issue. In addition, studies correlating the imaging findings with histology are necessary, in order to validate our results.

Acknowledgements

This publication was made possible by grants numbers R01LM007861, R01GM074068, U41RR019703, P01CA67165, and P41RR12318 from the National Institutes of Health (NIH), USA. Its contents are solely the responsibility of the authors and do not necessarily represent the official views of the NIH.

The authors would like to acknowledge Dr. S. Maier for the design and maintenance of the line scan diffusion sequence used to acquire data for the present study, as well as Dr. C.-F. Westin and the members of the Laboratory for

Mathematics in Imaging at Brigham and Women's Hospital Boston for the design and implementation of the 3D-tractography algorithm.

References

1. Central Brain Tumor Registry of The United States. Statistical Report: Primary Brain Tumors in The United States 1998–2002. Primary Brain Tumors in The United States 1998–2002. 2005. <http://cbtrus.org/reports//2005–2006/2006report.pdf>
2. Nicolato A, Gerosa MA, Fina P, Iuzzolino P, et al. Prognostic factors in low-grade supratentorial astrocytomas: a uni-multivariate statistical analysis in 76 surgically treated adult patients. *Surg Neurol* 1995;44(3):208–221. [PubMed: 8545771]discussion 221-3
3. Pignatti F, van den Bent M, Curran D, Debruyne C, et al. Prognostic factors for survival in adult patients with cerebral low-grade glioma. *J Clin Oncol* 2002;20(8):2076–2084. [PubMed: 11956268]
4. Janny P, Cure H, Mohr M, Heldt N, et al. Low grade supratentorial astrocytomas. Management and prognostic factors. *Cancer* 1994;73(7):1937–1945. [PubMed: 8137221]
5. Keles GE, Lamborn KR, Berger MS. Low-grade hemispheric gliomas in adults: a critical review of extent of resection as a factor influencing outcome. *J Neurosurg* 2001;95(5):735–745. [PubMed: 11702861]
6. Claus EB, Black PM. Survival rates and patterns of care for patients diagnosed with supratentorial low-grade gliomas: data from the SEER program 1973–2001. *Cancer* 2006;106(6):1358–1363. [PubMed: 16470608]
7. Mori S, van Zijl PC. Fiber tracking: principles and strategies - a technical review. *NMR Biomed* 2002;15(7–8):468–480. [PubMed: 12489096]
8. Lowe MJ, Horenstein C, Hirsch JG, Marrie RA, et al. Functional pathway-defined MRI diffusion measures reveal increased transverse diffusivity of water in multiple sclerosis. *Neuroimage* 2006;32(3):1127–1133. [PubMed: 16798013]
9. Kealey SM, Kim Y, Whiting WL, Madden DJ, et al. Determination of multiple sclerosis plaque size with diffusion-tensor MR Imaging: comparison study with healthy volunteers. *Radiology* 2005;236(2):615–620. [PubMed: 16040917]
10. Witwer BP, Moftakhar R, Hasan KM, Deshmukh P, et al. Diffusion-tensor imaging of white matter tracts in patients with cerebral neoplasm. *J Neurosurg* 2002;97(3):568–575. [PubMed: 12296640]
11. Mori S, Frederiksen K, van Zijl PC, Stieltjes B, et al. Brain white matter anatomy of tumor patients evaluated with diffusion tensor imaging. *Ann Neurol* 2002;51(3):377–380. [PubMed: 11891834]
12. Inoue T, Ogasawara K, Beppu T, Ogawa A, et al. Diffusion tensor imaging for preoperative evaluation of tumor grade in gliomas. *Clin Neurol Neurosurg* 2005;107(3):174–180. [PubMed: 15823671]
13. Goebell E, Paustenbach S, Vaeterlein O, Ding XQ, et al. Low-grade and anaplastic gliomas: differences in architecture evaluated with diffusion-tensor MR imaging. *Radiology* 2006;239(1):217–222. [PubMed: 16484348]
14. Mandonnet E, Capelle L, Duffau H. Extension of paralimbic low grade gliomas: toward an anatomical classification based on white matter invasion patterns. *J Neurooncol* 2006;78(2):179–185. [PubMed: 16739029]
15. Gering DT, Nabavi A, Kikinis R, Hata N, et al. An integrated visualization system for surgical planning and guidance using image fusion and an open MR. *J Magn Reson Imaging* 2001;13(6):967–975. [PubMed: 11382961]
16. Wells WM 3rd, Viola P, Atsumi H, Nakajima S, et al. Multi-modal volume registration by maximization of mutual information. *Med Image Anal* 1996;1(1):35–51. [PubMed: 9873920]
17. West J, Fitzpatrick JM, Wang MY, Dawant BM, et al. Comparison and evaluation of retrospective intermodality brain image registration techniques. *J Comput Assist Tomogr* 1997;21(4):554–566. [PubMed: 9216759]
18. Nimsky C, Fujita A, Ganslandt O, Von Keller B, et al. Volumetric assessment of glioma removal by intraoperative high-field magnetic resonance imaging. *Neurosurgery* 2004;55(2):358–371. [PubMed: 15271242]discussion 370-1

19. Dumas-Duport C, Varlet P, Tucker ML, Beuvon F, et al. Oligodendrogliomas. Part I: Patterns of growth, histological diagnosis, clinical and imaging correlations: a study of 153 cases. *J Neurooncol* 1997;34(1):37–59. [PubMed: 9210052]
20. Kelly PJ, Dumas-Duport C, Kispert DB, Kall BA, et al. Imaging-based stereotaxic serial biopsies in untreated intracranial glial neoplasms. *J Neurosurg* 1987;66(6):865–874. [PubMed: 3033172]
21. Price SJ, Jena R, Burnet NG, Hutchinson PJ, et al. Improved delineation of glioma margins and regions of infiltration with the use of diffusion tensor imaging: an image-guided biopsy study. *AJNR Am J Neuroradiol* 2006;27(9):1969–1974. [PubMed: 17032877]
22. Provenzale JM, McGraw P, Mhatre P, Guo AC, et al. Peritumoral brain regions in gliomas and meningiomas: investigation with isotropic diffusion-weighted MR imaging and diffusion-tensor MR imaging. *Radiology* 2004;232(2):451–460. [PubMed: 15215555]
23. Peled S, Gudbjartsson H, Westin CF, Kikinis R, et al. Magnetic resonance imaging shows orientation and asymmetry of white matter fiber tracts. *Brain Res* 1998;780(1):27–33. [PubMed: 9473573]
24. Westin CF, Maier SE, Mamata H, Nabavi A, et al. Processing and visualization for diffusion tensor MRI. *Med Image Anal* 2002;6(2):93–108. [PubMed: 12044998]
25. Ojemann JG, Miller JW, Silbergeld DL. Preserved function in brain invaded by tumor. *Neurosurgery* 1996;39(2):253–258. [PubMed: 8832661]discussion 258-9
26. Schiffbauer H, Berger MS, Ferrari P, Freudenstein D, et al. Preoperative magnetic source imaging for brain tumor surgery: a quantitative comparison with intraoperative sensory and motor mapping. *J Neurosurg* 2002;97(6):1333–1342. [PubMed: 12507131]
27. Skirboll SS, Ojemann GA, Berger MS, Lettich E, et al. Functional cortex and subcortical white matter located within gliomas. *Neurosurgery* 1996;38(4):678–684. [PubMed: 8692384]discussion 684-5
28. Nimsy C, Ganslandt O, Fahlbusch R. Implementation of fiber tract navigation. *Neurosurgery* 2006;58(4 Suppl 2):ONS292–ONS304.
29. Talos IF, Zou KH, Ohno-Machado L, Bhagwat JG, et al. Supratentorial Low-Grade Glioma Resectability: Statistical Predictive Analysis Based on Anatomic MR Features and Tumor Characteristics. *Radiology* 2006;239(2):506–513. [PubMed: 16641355]

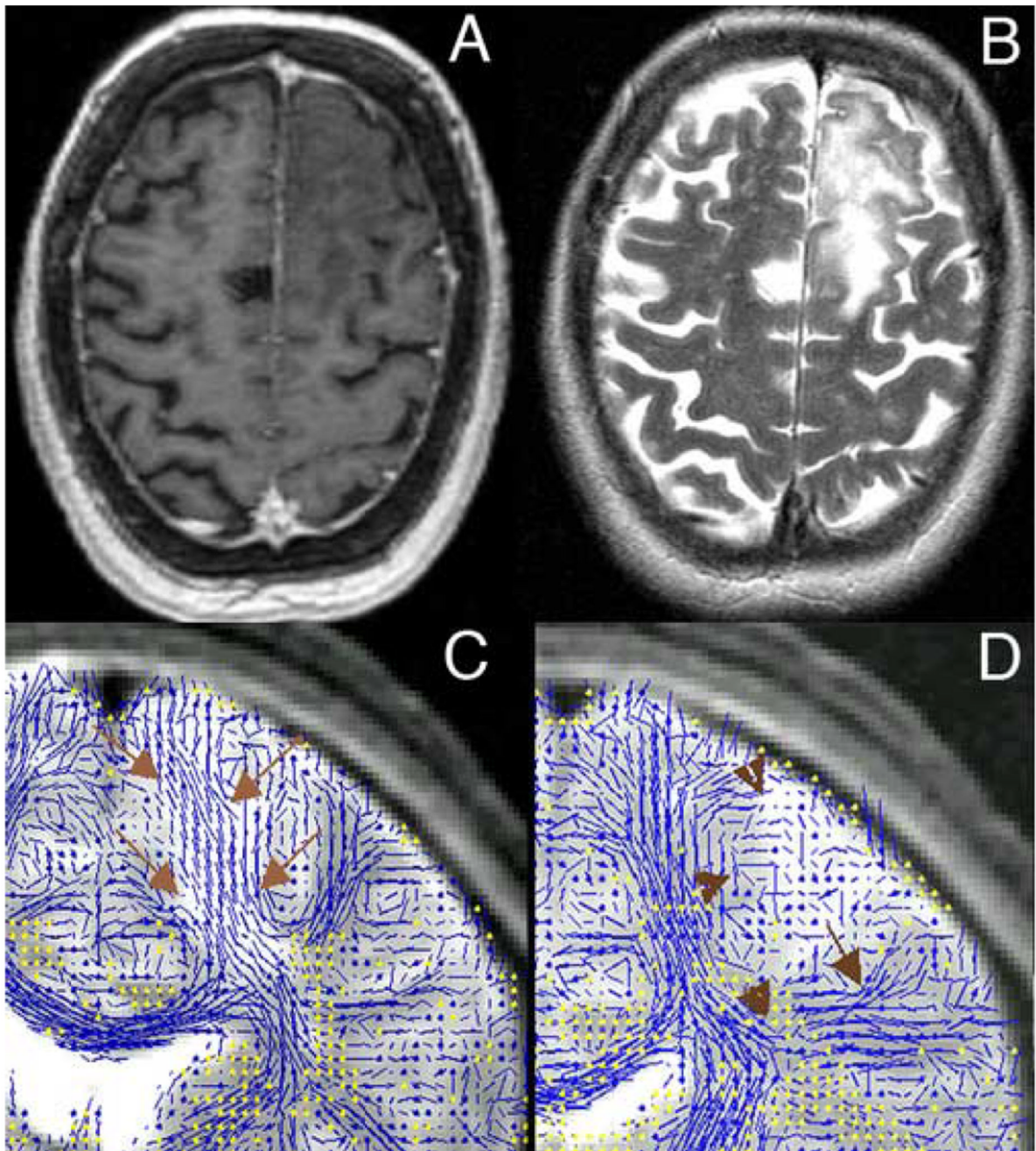


Figure 1.

Left frontal Oligodendroglioma WHO II. A: post-contrast, axial 3D-SPGR; B: axial T2-FSE; C: coronal view at the level of the posterior limb of the internal capsule; 2D-DT-MRI visualization overlaid on the corresponding T2-weighted baseline slice (the lines represent the in-plane fibers, whereas the through-plane fibers are represented as yellow dots); note the tumor infiltration of descending fibers (arrows); D: coronal view at a level located posterior from the slice in Figure 1C; fiber tracts in this area are displaced by the tumor mass (arrowheads).

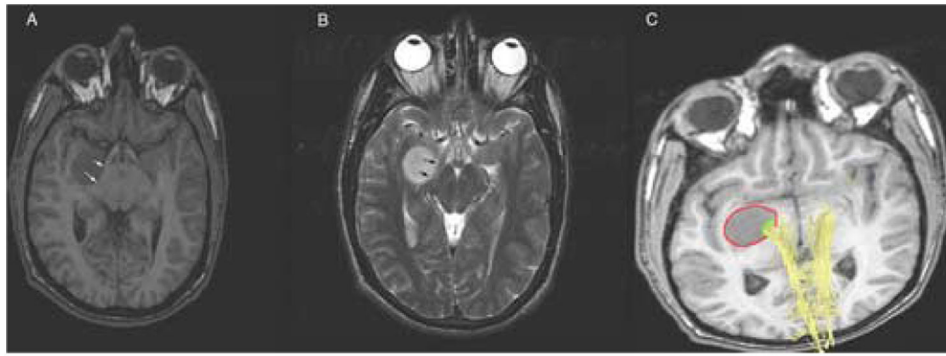


Figure 2.

Right temporal ganglioglioma. A: axial 3D-SPGR; B: axial T2-FSE; the tumor exerts mass effect on the right cerebral peduncle and right optic tract (arrows); C: 3D-tractography registered with the 3D-SPGR scan; corticospinal fibers (yellow) traversing the medial aspect of the tumor; red: manual segmentation of the tumor mass; green: manual segmentation of the tumor region intersected by corticospinal fibers.

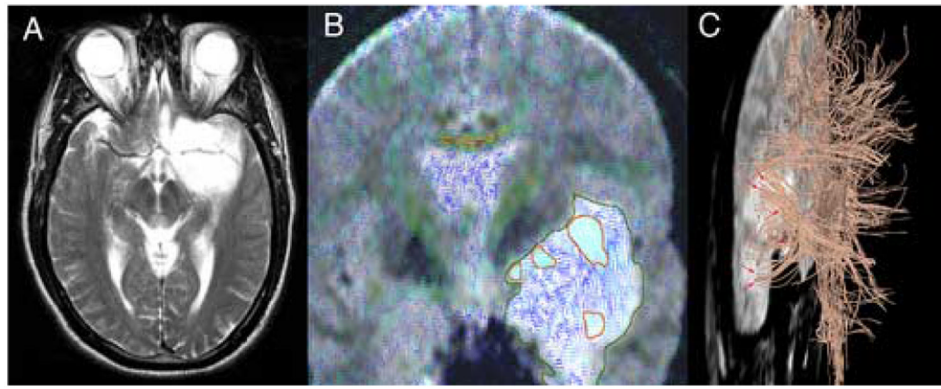


Figure 3. Left fronto-temporal Oligodendroglioma WHO II. A: axial T2-FSE; B: color-coded 2D-DT-MRI visualization overlaid on the corresponding T2-weighted slice; the tumor is outlined in dark green; areas of high fractional anisotropy (light-blue lines) within the tumor confines, corresponding to infiltrated white matter fibers, are outlined in red; C: 3D-tractography overlaid on the baseline T2-weighted acquisition (left lateral view); note the uncinus fasciculus (arrows) running through the T2-hyperintense tumor mass.

Table 1

Patient population and tumor characteristics

Case No.	Sex, Age (yrs.)	Tumor location	Histopathology	Eloquent cortical and white matter areas affected
1	F 33	L frontal	Astrocytoma WHO II	SMA, motor strip, motor pathway
2	F 34	R temporal	Oligodendroglioma WHO II	Wernicke's area, optic radiation
3	F 62	L frontal	Oligodendroglioma WHO II	SMA, motor pathway
4	M 62	R frontal medial	Anaplastic Astrocytoma	Motor strip, motor pathway
5	M 38	L frontal	Astrocytoma WHO II	Motor strip, motor pathway
6	F 45	L fronto-parietal	Anaplastic strocytoma	Motor and sensory strip, motor pathway, arcuate (superior longitudinal) fasciculus
7	F 46	R occipital	Oligodendroglioma WHO II	Optic radiation
8	M 23	R insular	Ganglioglioma	Motor pathway, uncinata fasciculus
9	F 18	R frontal	Anaplastic Astrocytoma (WHO III)	Motor strip, motor pathway
10	M 49	L frontal	Oligodendroglioma WHO II	SMA, motor pathway, corpus callosum
11	M 47	L fronto-temporal	Mixed Oligoastrocytoma WHO II	Broca's area, uncinata fasciculus
12	F 56	L fronto-parietal	Oligodendroglioma WHO II	Motor and sensory strip, motor pathway, arcuate fasciculus

Table 2

Volumetric assessment of white matter infiltration

Case No.	Tumor volume (ml)	Tumor volume infiltrating fiber tracts (ml)	Fraction of Tumor volume infiltrating fiber tracts (% of total tumor volume)
1	33.7	4.8	14.2
2	51.3	13.7	26.7
3	32.3	2.4	7.4
4	9.3	2.6	28.0
5	28.3	3.5	12.4
6	62.6	23.1	36.9
7	9.2	2.6	28.3
8	13.0	2.0	15.4
9	91.8	22.6	24.6
10	87.7	30.7	35.0
11	52.8	5.7	10.8
12	70	12.8	18.3